

## Thermal evaporation furnace with improved configuration for growing nanostructured inorganic materials

E. Joanni, R. Savu, L. Valadares, M. Cilense, and M. A. Zaghete

Citation: *Rev. Sci. Instrum.* **82**, 065101 (2011); doi: 10.1063/1.3597577

View online: <http://dx.doi.org/10.1063/1.3597577>

View Table of Contents: <http://rsi.aip.org/resource/1/RSINAK/v82/i6>

Published by the [AIP Publishing LLC](#).

---

### Additional information on *Rev. Sci. Instrum.*

Journal Homepage: <http://rsi.aip.org>

Journal Information: [http://rsi.aip.org/about/about\\_the\\_journal](http://rsi.aip.org/about/about_the_journal)

Top downloads: [http://rsi.aip.org/features/most\\_downloaded](http://rsi.aip.org/features/most_downloaded)

Information for Authors: <http://rsi.aip.org/authors>

## ADVERTISEMENT



**JANIS**

**Janis Dilution Refrigerators & Helium-3 Cryostats  
for Sub-Kelvin SPM**

Click here for more info [www.janis.com/UHV-ULT-SPM.aspx](http://www.janis.com/UHV-ULT-SPM.aspx)

# Thermal evaporation furnace with improved configuration for growing nanostructured inorganic materials

E. Joanni,<sup>1,a)</sup> R. Savu,<sup>2,3</sup> L. Valadares,<sup>4</sup> M. Cilense,<sup>2</sup> and M. A. Zaghete<sup>2</sup>

<sup>1</sup>*Centro de Tecnologia da Informação Renato Archer – CTI, Rod. Dom Pedro I km 143.6, 13069-901, Campinas, SP, Brasil*

<sup>2</sup>*Departamento de Físico-Química, Instituto de Química de Araraquara, Universidade Estadual Paulista – UNESP, Rua Prof. Francisco Degni s/n, 14800-900, Araraquara SP, Brasil*

<sup>3</sup>*Centro de Componentes Semicondutores – CCS, Universidade de Campinas – UNICAMP, C.P. 6061, Rua João Pandia Calógeras, 90, 13083-870, Campinas, SP, Brasil*

<sup>4</sup>*Instituto de Química – UNICAMP, C.P. 6154, 13084-971, Campinas, SP, Brazil*

(Received 8 November 2010; accepted 10 May 2011; published online 6 June 2011)

A tubular furnace specifically designed for growing nanostructured materials is presented in this work. The configuration allows an accurate control of evaporation temperature, substrate temperature, total pressure, oxygen partial pressure, volumetric flow and source-substrate distance, with the possibility of performing both downstream and upstream depositions. In order to illustrate the versatility of the equipment, the furnace was used for growing semiconducting oxide nanostructures under different deposition conditions. Highly crystalline indium oxide nanowires with different morphologies were synthesized by evaporating mixtures of indium oxide and graphite powders with different mass ratios at temperatures between 900 °C and 1050 °C. The nanostructured layers were deposited onto oxidized silicon substrates with patterned gold catalyst in the temperature range from 600 °C to 900 °C. Gas sensors based on these nanowires exhibited enhanced sensitivity towards oxygen, with good response and recovery times. © 2011 American Institute of Physics. [doi:10.1063/1.3597577]

## I. INTRODUCTION

For the last few years, progress in nanotechnology has led to the synthesis and characterization of a variety of nanostructures, i.e., nanowires, nanorods, nanotubes, using a wide range of materials such as metals,<sup>1</sup> carbides,<sup>2</sup> nitrides,<sup>3</sup> and oxides.<sup>4</sup> These nanometer-scale structures often possess enhanced optical and electrical characteristics due to quantum confinement effects, as well as high surface-to-volume ratios,<sup>4,5</sup> offering great prospects as building blocks in electronic and photonic devices. Morphology, dimensions, uniformity, growth direction and crystallinity are crucial factors during the synthesis of nanostructures, as these parameters will ultimately dictate their functionality.<sup>4-6</sup>

Some of the methods more frequently reported for the synthesis of semiconducting oxide nanostructures, both in powder and thin film forms, include chemical bath deposition,<sup>7</sup> hydrothermal synthesis,<sup>8</sup> chemical vapor deposition,<sup>9</sup> thermal evaporation,<sup>10,11</sup> sputtering,<sup>12</sup> and laser ablation.<sup>13</sup>

Among the physical deposition methods, the thermal evaporation (also called carbothermal reduction) is widely employed in nanofabrication processes due to its low cost, high yield, and easy implementation.<sup>6,10,11</sup> In spite of the popularity of this technique, most of the results reported until now were not obtained through an accurate control of the deposition process. The most common configurations used for thermal evaporation are either to locate the substrate at a certain distance from the source<sup>10</sup> or to place the substrate over the

boat containing the raw materials.<sup>11</sup> Both approaches have problems, since in the first case the substrate temperature is only approximately known (and includes a thermal gradient along the substrate) and, in the second one, the evaporation and deposition temperatures are the same. In both schemes the substrate temperature and source-substrate distance are not necessarily optimized or even compatible.

Works reporting the construction of vacuum furnaces with different configurations for attending a variety of research lines were already published.<sup>14-16</sup> van Laake *et al.* designed and fabricated a simple, low-cost reactor based on resistive heating of a suspended silicon platform for carbon nanotube synthesis.<sup>15</sup> Their results are encouraging, with the possibility of expanding the use of the CVD furnace for other applications such as the anisotropic growth of semiconducting oxides. However, the cost of building the reactor, as well as its maintenance, can be considered high for some research groups and the equipment demands delicate handling.

Schroer *et al.* developed two reactor designs for growing InAs nanowires.<sup>16</sup> Their hot wall reactor is based on a quartz tube furnace, being inexpensive and easy to mount and handle. Nevertheless, anisotropic growth can only be achieved for a narrow range of operating conditions. For improving nanostructure quality and increasing substrate coverage, the authors built a UHV cold wall reactor with a base pressure around 10<sup>-9</sup> Torr. On the other hand, this solution raised the equipment costs to high levels, as acknowledged by the authors themselves.<sup>16</sup>

Having in mind that nanotechnology represents an important research area and that the thermal evaporation method is one of the main techniques used for fabricating nanostructures, a better controlled process is urgently needed in order

<sup>a)</sup> Author to whom correspondence should be addressed. Electronic mail: ednan.joanni@cti.gov.br.

to achieve reproducible results that can be easily compared. In this work we report a new and simple configuration for the traditional thermal evaporation furnace that allows an accurate control of all the synthesis parameters. By adding a ceramic support that incorporates a substrate heater and a thermocouple, it becomes easy to set the desired evaporation and deposition temperatures and source-substrate distance. Moreover, these parameters become independent from each other, considerably increasing the number of controlled variables and, consequently, improving the flexibility of the process. The system also allows the independent control of gas flow, composition, and pressure as well as the deposition of nanostructures either downstream or against the gas flow. Using this setup, highly crystalline semiconducting oxide nanowires with different morphologies were synthesized and their gas sensing properties were investigated.

## II. EXPERIMENTAL DETAILS

### A. Description of the evaporation system

The complete system, shown in Fig. 1(a), can be divided in two subsystems: one for atmosphere control and another for temperature management. The gas composition and flow are set by two volumetric flow controllers (one for oxygen and one for inert gases). The pressure is determined by a pressure sensor, diaphragm and up-to-air valves mounted in a 4-way cross and connected to a rotary vacuum pump. Tubes for gas introduction and pumping complete this subsystem. The configuration shown in Fig. 1 allows for downstream depositions; by reversing the tube placements, upstream depositions can also be performed. The evaporation is carried out in a tubular furnace with a single hot zone (EDG model FT-HV/20/10P)

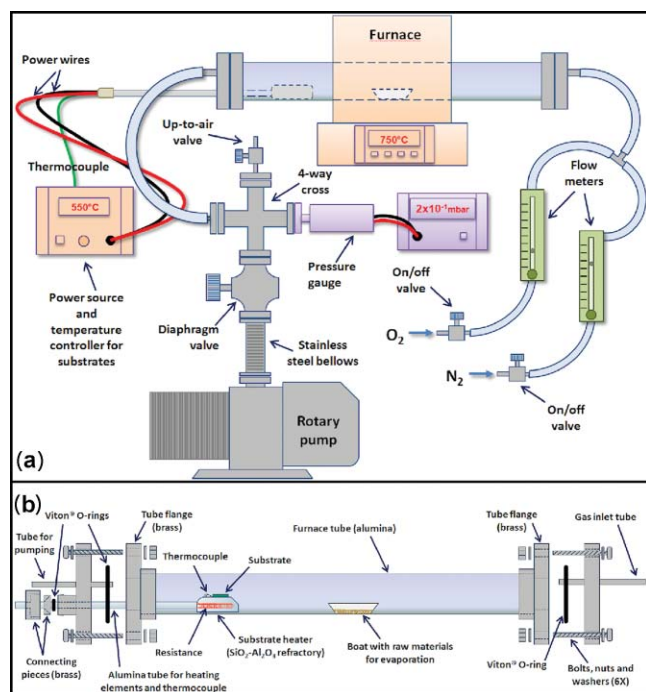


FIG. 1. (Color online) Schematic drawings of (a) the complete system for growing oxide nanostructures by thermal evaporation and (b) the tube assembly and the substrate holder.

and equipped with a programmable temperature controller. A substrate holder provided with a separate heating system and temperature control allows the independent setting of evaporation and deposition temperatures.

Figure 1(b) shows a schematic drawing of the alumina tube where the actual nanostructural growth takes place. The tube is fitted with brass flanges held in place with high temperature silicone-based adhesive. The mating flanges incorporate inlet and outlet tubes for gas flow and a custom-designed coupling that allows the sample holder to be translated while maintaining a vacuum-tight connection. Viton® o-rings are used for ensuring the hermetic sealing at all the interfaces. The sample holder was assembled from an aluminosilicate ceramic piece for supporting the substrates and an alumina tube of approximately 1 m length and 1.5 cm diameter having four through-holes for the thermocouple and electrical resistance connections. By using a single-zone furnace having a hot region of small dimensions when compared to the length of the tube, we were able to control the substrate temperature independently from the evaporation temperature. This was achieved by varying the distance between the substrate holder and the center of the tubular furnace (i.e., between the substrate and the evaporation source). As a consequence, even though the furnace and substrate holder have their own controllers, the maximum difference between evaporation and deposition temperatures depends on the distance between the raw materials and the substrate. For example, if the source-substrate distance is too small, these temperatures will necessarily be similar.

In the process of building the substrate heater, a series of channels approximately 1 cm deep and 0.5 cm wide were excavated in the porous ceramic in order to accommodate the electrical resistance. The type K thermocouple and the connection wires for electrical supply of the Ni-Cr resistance were introduced inside the thin alumina tube. Subsequently, the ceramic piece was attached to this alumina tube using high temperature alumina cement. Next, the heater was coated with a thin cement layer in order to assure electrical insulation of the resistance, preventing also any chemical reaction with the evaporated materials.

### B. System operation

The procedure for growing oxide nanostructures begins by loading the raw materials in a ceramic boat. The precursors are either metal granules, or mixtures of a finely ground oxide with a reducing agent (normally graphite). After placing the boat at the hot zone of the furnace, the substrates are positioned on the sample holder, the distance between the boat and the sample holder is adjusted to the desired value, the flanges are closed and the tube is sealed by tightening the screws. At this point, the evaporation and deposition temperatures are set and both heaters are turned on. The vacuum pump is then started and the diaphragm valve is fully open in order to evacuate the tube up to its base pressure ( $5 \times 10^{-2}$  mbar in our case). This step is necessary for removing the humidity and other gases adsorbed in the raw materials and on the internal surface of the tube. When the desired temperatures were reached, the valves controlling the flow of gases were

opened and the deposition pressure was adjusted by regulating the diaphragm valve. When the deposition time was completed, the heaters and the gas flow were turned off and the system was allowed to cool down.

### C. Synthesis of semiconducting oxide nanowires and configuration of the gas sensors

By varying the source-substrate distance, the deposition pressure, the gas flow, the percentage of oxygen and the substrate temperature, we were able to fabricate tin oxide nanowires, nano-plates, and nano-ribbons, indium oxide nanowires and highly branched indium tin oxide nanowires. This demonstrates that the equipment is suitable for growing different inorganic materials in nanostructured form.

The procedure and results presented below refer to the growth of indium oxide nanowires using three source-substrate distances and four substrate temperatures, with all depositions being performed in the direction of the gas flow. Oxidized silicon, patterned with 160 nm thick gold catalyst dots, was used as substrates. The catalyst dots were deposited by DC sputtering through a shadow mask having an array of holes with a diameter of 172  $\mu\text{m}$ . Depositions of indium oxide nanostructures used as raw materials a mixture of indium oxide ( $\text{In}_2\text{O}_3$  – 99.9% purity, Alfa Aesar) and graphite powders. Usually, the graphite is added to the oxide powder in order to lower its evaporation temperature. Using a rotary pump and volumetric flow controllers (between 100 and 200 sccm total flow), an atmosphere composed of 90%  $\text{N}_2$  and 10%  $\text{O}_2$  or of pure nitrogen was employed and the deposition pressure was kept between 2 and 10 Torr. The source-substrate distance was adjusted between 8 and 13.5 cm, with the evaporation time being varied in the range from 30 to 180 min. The deposition temperature, controlled independently of the evaporation temperature (900–1050  $^\circ\text{C}$ ), was varied between 600 and 900  $^\circ\text{C}$ . The complete set of parameters used in this work is presented in Table I.

After deposition, the degree of crystallinity and the phases present in the samples were analyzed by x-ray diffraction (XRD – Rigaku Rint 2000), the growth direction of the nanostructures was studied by transmission electron microscopy (TEM – Jeol JEM 2100), and their morphology was

TABLE I. Complete set of parameters used for the evaporation process of indium oxide nanowires.

Sample	IE1	IE2	IE3	IE4	IE5
Indium oxide (g)	0.2	0.5	0.2	0.2	0.2
Graphite (g)	0.4	0.5	0.1	0.1	0.1
Source-substrate distance (cm)	13.5	10	8	8	8
Substrate temperature ( $^\circ\text{C}$ )	600	900	625	700	700
Evaporation temperature ( $^\circ\text{C}$ )	1000	1050	900	900	1000
Pressure(Torr)	7.5	2	10	10	10
$\text{N}_2$ flow (sccm)	180	180	90	100	100
$\text{O}_2$ flow (sccm)	20	20	10	...	...
Evaporation time (min)	120	30	60	180	60

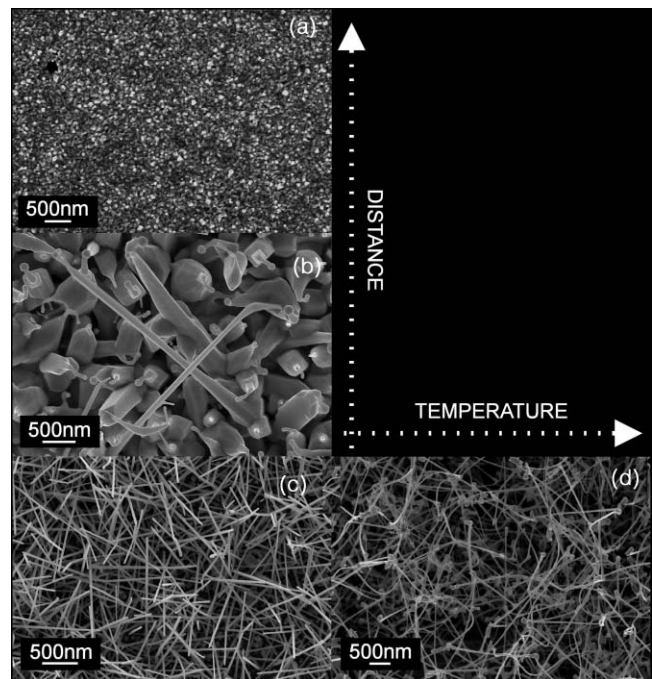


FIG. 2. FE-SEM surface images for the (a) IE1, (b) IE2, (c) IE3, and (d) IE4 indium oxide nanostructured films.

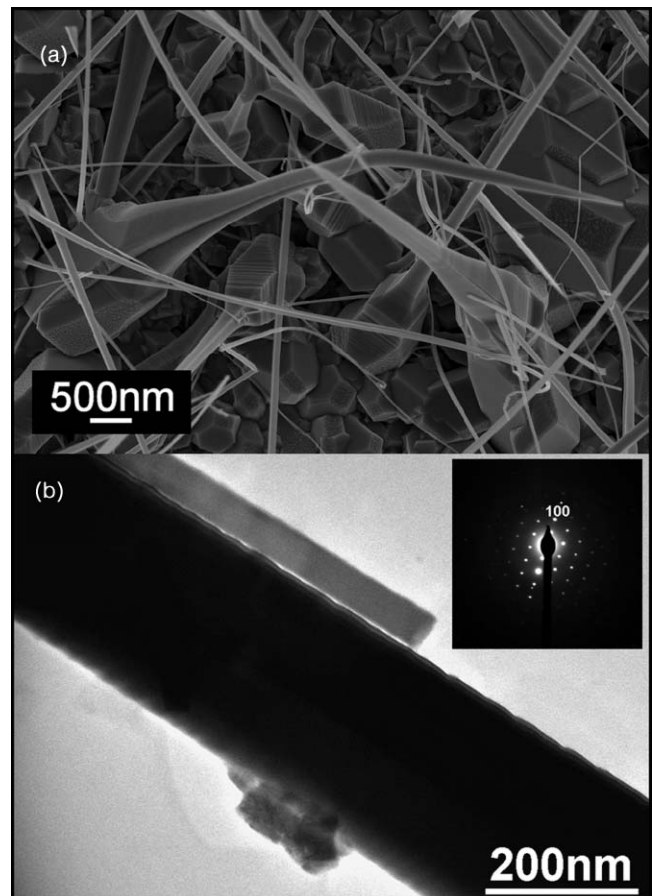


FIG. 3. (a) FE-SEM surface image for the IE5 sample and (b) TEM image of an individual nanowire broken from the same sample. The inset shows a selected area electron diffraction pattern (SAED) taken perpendicular to the long axis of the wire indicating the (100) growth direction.

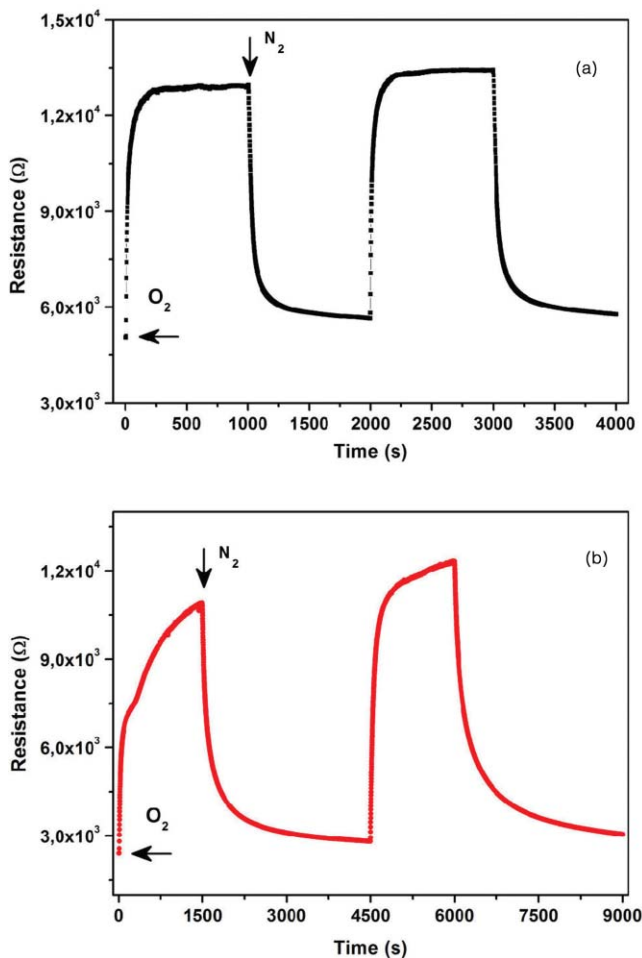


FIG. 4. (Color online) Gas sensing response towards oxygen for (a) the IE3 and (b) IE4 nanostructured gas sensors working at a temperature of 300 °C.

assessed by field emission scanning electron microscopy (FE-SEM – Zeiss Supra 35).

The sensitivity towards oxygen of the as-deposited samples was tested at different working temperatures. This was possible due to the fact that the gold dots, besides their catalytic activity, also served as contact electrodes, making it possible to record the changes in resistance of the nanowires that bridged the gap between adjacent gold dots. For the electrical resistance measurements, the samples were maintained in nitrogen atmosphere (100 sccm  $N_2$ ) until the temperature was stabilized; at this point the nitrogen flow was stopped, 100 sccm  $O_2$  was injected into the chamber and the measurements were started. The samples were submitted to four consecutive oxygen/nitrogen cycles, using a working temperature of 300 °C. The measurements were performed by means of an electrochemical interface (Solartron 1287), applying a 0.5 V potential difference.

### III. RESULTS AND DISCUSSION

Figure 2 presents surface FE-SEM images of the indium oxide nanostructured films as a function of the source-substrate distance and deposition temperature, samples IE1 (Fig. 2(a)), IE2 (Fig. 2(b)), IE3 (Fig. 2(c)), and IE4

(Fig. 2(d)). Decreasing the source-substrate distance from 13.5 to 8 cm, the film morphology changes from continuous dense layer (Fig. 2(a)), to large crystals with nanowires at their tips (Fig. 2(b)) to a highly uniform nanowire array (Fig. 2(c)). At a deposition distance of 13.5 cm, a dense layer was obtained, with no indication for nanostructural nucleation. This is mainly due to the low substrate temperature used for the deposition. For a source-substrate distance of 10 cm and a deposition temperature of 900 °C, nanowires having a tip diameter of 100 nm with a very large base (Fig. 2(b)) and a length of a few microns were grown. Their substrate coverage density is low, and their size is not uniform. Furthermore, these nanowires are not preferentially oriented in relation to the substrate and their morphology indicates a large amount of liquid material during deposition. This is due to the low deposition pressure (2 Torr) and high evaporation and substrate temperatures (1050 °C and 900 °C, respectively). At this evaporation temperature the vapor pressure of indium is  $\sim 5 \times 10^{-2}$  Torr, generating a larger amount of material arriving on the substrate than for a deposition pressure of 10 Torr. All the nanowires have spheres at the tips indicating that under these conditions the growth mechanism is Vapor-Liquid-Solid (VLS). According to this mechanism, the nanowires grow by precipitation from droplets of super-saturated molten material present on the heated substrate surface.<sup>4,5,17</sup> By decreasing the target-substrate distance to 8 cm and the substrate temperature to 625 °C, morphologically uniform and interconnected thin nanowires were obtained at a deposition pressure of 10 Torr (Fig. 2(c)). Even for a low deposition temperature, by decreasing the source-substrate distance, it is possible to trigger the nucleation and the growth of nanowires. The structures present widths of 30 nm and lengths of around 1  $\mu m$ . Very fine catalytic particles are still present at their tips, indicating the growing mechanism as being VLS. The substrate coverage density increased to approximately 76 wires/ $\mu m^2$ . By increasing the substrate temperature to 700 °C the film morphology was not significantly affected. Nanowires with high substrate coverage and a diameter of 100 nm were obtained. Still, comparing the IE3 and IE4 samples, one can observe that for the 700 °C deposition temperature the nanostructures are longer in length, thinner and present catalytic particles with higher diameter at their tips. It is clear that this is due to the lack of oxygen during growth, leading to a higher amount of liquid phase at the substrate surface. Moreover, the deposition time for the IE4 sample was three times higher than for the IE3, resulting in a slight change in nanowire morphology.

Using the same deposition time as for the IE3 sample, but higher evaporation and deposition temperatures and pure nitrogen atmosphere (IE5), nanowires with a large base and fine tips were obtained (Fig. 3(a)). The nanostructures have average lengths of 7  $\mu m$ , tapering along their length until reaching a diameter smaller than 100 nm at the tips. The results indicate the growing mechanism as being Vapor-Solid (VS). According to the literature, this mechanism is based on the condensation of evaporated material onto the substrate positioned in a lower temperature region, with the nanowires nucleating from these sites.<sup>5,18,19</sup> Figure 3(b) presents a TEM image of an individual needle broken from the IE5 sample. The nanowire is single crystalline, faceted, with a square cross section, reflect-

ing the cubic crystalline structure of indium oxide. The SAED pattern taken perpendicular to the long axis of the nanowire (Inset Fig. 3(b)), is consistent with the indexed patterns for the indium oxide with (100) growth direction.

Figure 4 shows the gas response towards oxygen for the IE3 (Fig. 4(a)) and IE4 (Fig. 4(b)) sensing devices. For the working temperature of 300 °C, the IE3 sensor exhibits a good reproducibility and a high stability for the four gas cycles performed. The sensibility (defined as the ratio between the resistance in O<sub>2</sub> and the resistance in N<sub>2</sub>) for this device is of 2.5 for the testing temperature used, with response and recovery times (defined as 90% of the final value in O<sub>2</sub> and N<sub>2</sub> atmospheres, respectively) of 1 and 3 min, respectively. Even though its sensibility is reasonable, the IE4 gas sensor presents a very slow response, not stabilizing for the same time interval used for testing. Moreover, its recovery is very slow, requiring more than double the testing time used for the IE3 sensing device. As the device does not stabilize in any of the gases used, the response and recovery times could not be determined. The initial low resistance of these devices can be due to the continuous layer at the base of the nanostructures that acts as a thin sensing film and contributes to the final sensing response.

#### IV. CONCLUSIONS

In this work we report the design and assembly of an evaporation furnace with improved configuration. By using a better control of the deposition parameters, nanostructures with different morphologies were obtained. The FE-SEM images of the indium oxide nanowires show that the structures grow either by VLS or VS mechanism, depending on the processing conditions. The TEM analysis indicated their high degree of crystallinity, with no grain boundaries along their length. The gas sensing devices based on these nanostructures shows good sensibility towards oxygen at a working temperature of 300 °C. The relatively short response time and good reproducibility of some of the gas sensors indicate that, with a controlled and low cost system, devices with high performance can be obtained.

The main contribution of this work is, to the best of our knowledge, the possibility to control, for the first time, all the major parameters involved in the growth of oxide

nanostructures by evaporation. Furthermore, variables which normally are interdependent (pressure and gas flow, evaporation temperature, and deposition temperature) become independently controllable. Other advantages of such evaporation system are the simple assembly, operational flexibility and low cost. The system offers good reproducibility, even for a large range of operation conditions, allowing the fabrication of nanostructures with different morphologies.

#### ACKNOWLEDGMENTS

R. Savu would like to acknowledge the financial support of FAPESP Brazilian foundation through her Ph.D. grant (Grant No. DD05/59270-0). All the authors acknowledge the financial support of FAPESP and CNPq Brazilian foundations.

- <sup>1</sup>L. Chen, K. Arakawa, and H. Mori, *Nanotechnology* **21**, 285304 (2010).
- <sup>2</sup>M. Yamaguchi, S. Ueno, R. Kumai, K. Kinoshita, T. Murai, T. Tomita, S. Matsuo, and S. Hashimoto, *Appl. Phys. A* **99**, 23 (2010).
- <sup>3</sup>M. U. Niemann, S. S. Srinivasan, A. R. Phani, A. Kumar, D. Y. Goswami, and E. K. Stefanakos, *J. Nanomater.* **2008**, 950967 (2008).
- <sup>4</sup>S. V. N. T. Kuchibhatla, A. S. Karakoti, D. Bera, and S. Seal, *Prog. Mater. Sci.* **52**, 699 (2007).
- <sup>5</sup>J. G. Lu, P. Chang, and Z. Fan, *Mater. Sci. Eng. R* **52**, 49 (2006).
- <sup>6</sup>Z. R. Dai, Z. W. Pan, and Z. L. Wang, *Adv. Funct. Mater.* **13**, 9 (2003).
- <sup>7</sup>B. Cao and W. Cai, *J. Phys. Chem. C* **112**, 680 (2008).
- <sup>8</sup>U. Pal and P. Santiago, *J. Phys. Chem. B* **109**, 15317 (2005).
- <sup>9</sup>Y. Hao, G. Meng, C. Ye, and L. Zhang, *Cryst. Growth Des.* **5**, 1617 (2005).
- <sup>10</sup>Z. R. Dai, Z. W. Pan, and Z. L. Wang, *J. Am. Chem. Soc.* **124**, 8673 (2002).
- <sup>11</sup>H. Jia, Y. Zhang, X. Chen, J. Shu, X. Luo, Z. Zhang, and D. Yu, *Appl. Phys. Lett.* **82**, 4146 (2003).
- <sup>12</sup>K. W. Cheng, Y. T. Lin, C. Y. Chen, C. P. Hsiung, J. Y. Gan, J. W. Yeh, C. H. Hsieh, and L. J. Chou, *Appl. Phys. Lett.* **88**, 043115 (2006).
- <sup>13</sup>R. Savu and E. Joanni, *J. Mater. Sci.* **43**, 609 (2008).
- <sup>14</sup>C. C. Lee, D. T. Wang, and W. S. Choi, *Rev. Sci. Instrum.* **77**, 125104 (2006).
- <sup>15</sup>L. van Laake, A. J. Hart, and A. H. Slocum, *Rev. Sci. Instrum.* **78**, 083901 (2007).
- <sup>16</sup>M. D. Schroer, S. Y. Xu, A. M. Bergman, and J. R. Petta, *Rev. Sci. Instrum.* **81**, 023903 (2010).
- <sup>17</sup>P. Cheyssac, M. Sacilotti, and G. Patriarche, *J. Appl. Phys.* **100**, 044315 (2006).
- <sup>18</sup>E. Comini, C. Baratto, G. Faglia, M. Ferroni, A. Vomiero, and G. Sberveglieri, *Prog. Mater. Sci.* **54**, 1 (2009).
- <sup>19</sup>N. Wang, Y. Cai, and R. Q. Zhang, *Mater. Sci. Eng. R* **60**, 1 (2008).